Geometrical distortion calibration of the stereo camera for the BepiColombo mission to Mercury

Emanuele Simioni[a], Vania Da Deppo[a,b], Cristina Re[b] ,Giampiero Naletto[a,b,c], Elena Martellato[b], Donato Borrelli[d], Michele Dami[d], Gianluca Aroldi[d], Iacopo Ficai Veltroni[d], Gabriele Cremonese[b]

[a]CNR-Institute for Photonics and Nanotechnologies, Padova LUXOR, Padova, Italy , [b]INAF Astronomical Observatory Padova, Padova, Italy, [c]Department of Information Engineering, University of Padova, Padova, Italy, [d]LEONARDO Spa, Via A. Einstein, 35 ,50013 Campi Bisenzio (FI)

ABSTRACT

The ESA-JAXA mission BepiColombo that will be launched in 2018 is devoted to the observation of Mercury, the innermost planet of the Solar System. SIMBIOSYS is its remote sensing suite, which consists of three instruments: the High Resolution Imaging Channel (HRIC), the Visible and Infrared Hyperspectral Imager (VIHI), and the Stereo Imaging Channel (STC). The latter will provide the global three dimensional reconstruction of the Mercury surface, and it represents the first push-frame stereo camera on board of a space satellite.
Based on a new telescope design, STC combines the advantages of a compact single detector camera to the convenience of a double direction acquisition system; this solution allows to minimize mass and volume performing a push-frame imaging acquisition. The shared camera sensor is divided in six portions: four are covered with suitable filters; the others, one looking forward and one backwards with respect to nadir direction, are covered with a panchromatic filter supplying stereo image pairs of the planet surface. The main STC scientific requirements are to reconstruct in 3D the Mercury surface with a vertical accuracy better than 80 m and performing a global imaging with a grid size of 65 m along-track at the periherm.
Scope of this work is to present the on-ground geometric calibration pipeline for this original instrument.
The selected STC off-axis configuration forced to develop a new distortion map model.
Additional considerations are connected to the detector, a Si-Pin hybrid CMOS, which is characterized by a high fixed pattern noise. This had a great impact in pre-calibration phases compelling to use a not common approach to the definition of the spot centroids in the distortion calibration process.
This work presents the results obtained during the calibration of STC concerning the distortion analysis for three different temperatures. These results are then used to define the corresponding distortion model of the camera.

Keywords: space instrumentation, stereo-camera, distortion model, geometric calibration, push-frame

1. INTRODUCTION

BepiColombo is the fifth cornerstone mission of the European Space Agency (ESA). The launch campaign will start in July 2017 and the launch is foreseen in April 2018. The aim of the mission is the study of Mercury, the innermost planet of the Solar System [1]. The planet, reached for the first time by the Mariner 10 mission in 1974, presents a set of characteristics which makes it one of the most interesting and challenging target for planetary exploration.
The environmental condition of the planet due to proximity to the Sun, its orbital resonance, the particular composition of the surface, the presence of a magnetic field, and the absence of atmosphere make Mercury a perfect target for a multifunctional mission such as BepiColombo.
Two modules compose the BepiColombo satellite [2]: the ESA Mercury Planet Orbiter (MPO) [3], carrying remote sensing and radio science experiments, and the JAXA Mercury Magnetospheric Orbiter (MMO) [4]. SIMBIOSYS (Spectrometer

Space Telescopes and Instrumentation 2016: Optical, Infrared, and Millimeter Wave, edited by Howard A. MacEwen, Giovanni G. Fazio, Makenzie Lystrup, Proc. of SPIE Vol. 9904, 990410 · © 2016 SPIE · CCC code: 0277-786X/16/$18 · doi: 10.1117/12.2232639

and Imagers for MPO BepiColombo Integrated Observatory SYStem) is an integrated suite for imaging and spectroscopic investigation of the Mercury surface [7]. With a spectral band which covers wavelengths from UV to near infrared, the instrument incorporates three different channels: the STereoscopic imaging Channel, STC [8]; the High Resolution Imaging Channel, HRIC [11]; and the Visible and near-Infrared Hyperspectral Imager, VIHI [12].
STC is a stereo camera with multiple sub-channels which allows to acquire the surface of the planet from images in different directions and different wavelength bands. During the first six months of the mission, STC will perform the complete global mapping of the planetary surface with ground sample distance (GSD) of 65 m along-track at the periherm distance of 480 km. The STC channel will allow to generate Digital Terrain Models (DTM) with an upper limit of the vertical accuracy of 90 m at periherm. A particular validation setup [8,9] allowed, during the calibration process of the Flight Model (FM), to acquire on ground a series of stereo pairs and to demonstrate the possibility to improve the vertical accuracy by a factor two with respect to the requirement. The STC FM has been successfully tested at the Leonardo company premises in Campi Bisenzio (FI- Italy), where an ad-hoc Optical Ground Support Equipment (OGSE) has been developed to test and calibrate STC.
Because of the limited mass and power resources allocated for this instrument, an original off axis design was chosen for the STC camera. In this context, considering the high variations of the MPO thermal environment, which can cause a variation as large as 4% of the focal length as verified in MDIS (Mercury Dual Imaging System), an extremely detailed definition of the distortion map of the instrument is required. This work defines the distortion map of the instrument following two different approaches.

2. STC STEREO CHANNEL

STC is a double wide angle camera able to acquire simultaneously images from two different perspectives in the panchromatic filters providing stereo pairs with a stereo angle of ±21.35° with respect to the nadir.
While the panchromatic images will provide the data for the DTM generation, four additional different broadband filters will provide specific multispectral [18] images of selected Mercury regions.
The classical approach for stereo cameras is based on push broom acquisition mode with linear array sensors, taking advantage of the spacecraft movement along the orbit to generate bidimensional images.In the case of STC, a push-frame mode has been adopted using a single hybrid CMOS Active Pixel Sensor (APS) bi-dimensional array which acquires at the same time the forward and the backward fields of view covering 5.3° cross-track and of 3.2° along-track for each panchromatic filter. The selected APS produced by Raytheon Vision System (Goleta, CA, USA) has a snapshot image acquisition, allowing very short exposure times and limiting smearing problems.
The main instrument parameters and performances at periherm are shown in Table 1.

Table 1. Main performances of STC at periherm (considering two different orbits, corresponding to the first and last part of the global mapping mission phase, with the periherm respectively at 480 and 400 km).

	Spectral range (nm)	Boresight direction (°)	FOV (along track) (°)	Coverage (on-ground along track central scale factor | swath)				
				[pxl]	First orbits [m/px | km^2]		Last orbits [m/px | km^2]	
Panchromatic filter	700 ± 100	21.375	2.4	832×384	61.2	43.6×24.4	50.5	36.5×20.1
Other filters	420 ±10	19.22	0.8	832×64	58.8	43.9×3.8	48.6	36.7×3.2
	550 ± 10	19.22	0.8	832×64	58.8	43.9×3.8	48.6	36.7×3.2
	750 ± 10	17.95	0.8	832×64	57.7	43.8×3.9	47.6	36.6×3.2
	920 ± 10	17.95	0.8	832×64	57.7	43.8×3.9	47.6	36.6×3.2
Stereo accuracy upper limit (m)					90		80	

The STC optical configuration is shown in Figure 1. The optical elements are two flat folding mirrors which redirect the fields of view inclined by ±21.375° with respect to the camera "central axis" to a much smaller ±3.75° one. Then, a correcting doublet (with the same function of the classical Schmidt correcting plate) reduces the aberration introduced by the following primary mirror. All the optical paths after the correcting plate is common to both channels and represents an off-axis portion of a modified Schmidt design. The main optical parameters of STC are summarized in Table 2.

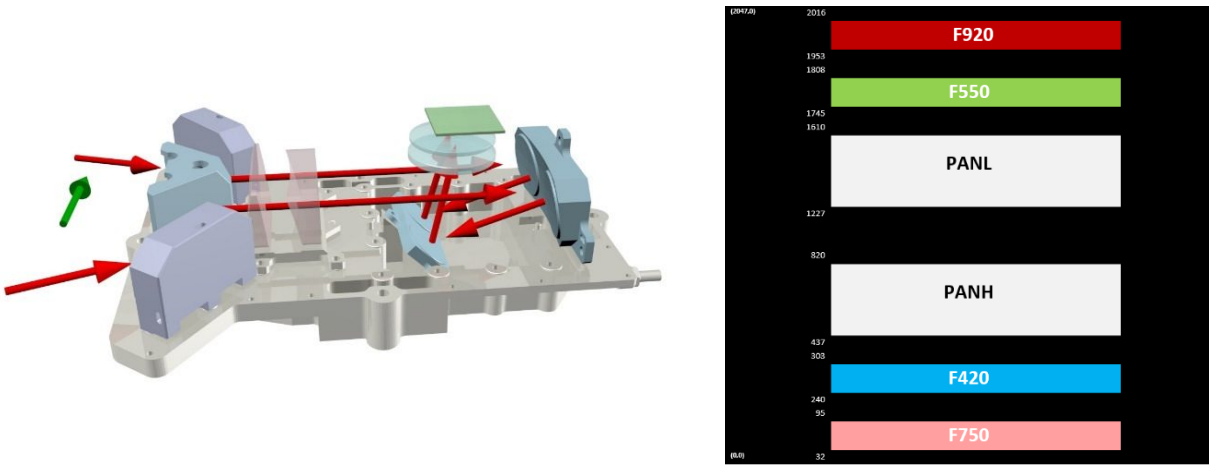

(a) (b)

Figure 1. (a) Optical path of STC. The green arrow represents the along track direction. The red arrows show the two optical paths initially differentiated with respect to nadir and then almost co-axial up to the detector. (b) Filter coverage on the sensor array. Lateral narrower filters are dedicated to multispectral color-mapping while the central ones to stereo acquisition.

The off-axis choice is justified by the need to have a free back focal length able to easily integrate the focal plane assembly (FPA) preserving the required optical performance.
The aperture stop position (in the front focal plane of the principal mirror) has been placed after the correcting doublet. This configuration was required by the filter choice: Filter Strip Assembly (FSA) needs the telecentricity of the design guaranteed to prevent wavelength shift.

Table 2. Principal optical parameters of STC.

Focal length	95.2 mm
Focal ratio	F/6.3
IFoV	23”/px
FoV (cross-track direction)	5.3°
MTF	0.65-0.69
PSF(FWHM)	1.36/1.45 pixels
Pupil size diameter	15 mm
Pixel size	10 µm

3. DISTORTION MAP MODEL

The geometric distortion depends on the optical configuration and can be determined theoretically by ray-tracing. As for STC, we are working with an original off-axis configuration which needs a new approach for the definition of the intrinsic parameters of the optical system.
The classical approach for the definition of the distortion map is the extraction of its component along the tangential and sagittal directions with an on-ground geometric calibration, then it will be corrected by in-flight stellar calibration. This approach is commonly applied to the pinhole cameras and demonstrates its robustness even for photogrammetric applications. A recent example is the Wide Angle Camera for the Rosetta mission [13] which allowed the 3D reconstruction of its cometary target [14] thanks to the definition of the distortion map of the camera (defined around 2.5% and 1% respectively in tangential and sagittal direction [16]). The thermal acquisition condition is another important issue that can affect the distortion model definition.

The case of the MESSENGER mission, also dedicated to the close observation of Mercury, is symbolic to explicate the sensitivity of the focal plane position to the thermal conditions. The assembly of the NAC for Mercury Dual Imaging System (MDIS) [17] has been in fact realized in all-aluminum to be able to withstand the intense thermal distortion over the operational temperature range of the instrument and allowing to respect the restricted distortion requirements of less than 1.28 pixels (residuals from the nominal position at the edge of the FoV) [17].
Since STC will also deal with extreme temperature conditions, the analysis of the distortion map as function of the thermal variations, is very important. Furthermore STC will has as mean goal the acquisition of the images for the global 3D reconstruction of the planet and the distortion model becomes mandatory for high accuracy DTM (Digital Terrain Model) generation
The three main factors contributing to the final vertical accuracy of the 3D products are (without considering the matching error in the image plane):

-the knowledge of the pointing of the cameras within the pivot plane
-the precision of the spacecraft attitude
-the knowledge of the cameras focal lengths and distortions

In the STC context, whose main task is the complete 3D reconstruction of Mercury surface, a very detailed analysis of the distortion map of the instrument is fundamental to define a minimal interpolation error on the images to be processed in the photogrammetric pipeline and to develop a model which could approximate the thermal distortion during different phases of the mission.
At the same time, STC is an off-axis instrument and thanks to the Schmidt design and to the aperture stop position, the distortion contribution is (as theoretical value) below the 0.3% over all the filters [8].

The distortion map describes the model of the residuals of the transformation between the 3D object coordinates and their projection on the camera image plane considering the pinhole camera model. By means of a suitable calibration campaign realized in Leonardo company (Campi Bisenzio, Italy), it has been possible to retrieve a great amount of information for a detailed definition of the STC distortion map.

Different approaches are historically used to calibrate a camera (even with a so particular design) as a pin-hole. As described in [6], the calibration of this model can be computed directly by images through specific algorithms. This approach was used during the stereo validation phase of the STC instrument [8]. The off axis configuration of STC on the other side do not allow to define nowadays a distortion map as classically defined in the imaging approaches.
By using the OGSE, the instrumental suite allows to have a great amount of information.
As described in Figure 2, the setup developed in Leonardo allows to retrieve two kinds of information:

-the direction of the light ray in entrance of the optical system for both the channels with a unique alignment.
-the projected position on the image planes.

These two sets of data allow to define the pin-hole model which maximizes the correlation between them defining the projective system of the instrument.

3.1 The Optical Ground Support Equipment

STC calibration activities were realized using an ad-hoc Optical Ground Support Equipment (OGSE) (see Figure 2) which integrates the facilities commonly exploited for the radiometric, geometric, and spectrometric calibration approaches.
Three different light selectable sources (a QTH lamp, a monochromator, an integrating sphere) had been exploited to illuminate a suitable target (either a pinhole or a diffuser). The light coming from the target is then collimated via a chromatically corrected lens system with a focal length of 750 mm. The collimated beam is directed into the camera via a plane folding mirror, working nominally with an inclination of 45°. The mounting base of the folding mirror is composed by two-axis rotators which allow to rotate the mirror in azimuth and elevation in order to redirect the collimated beam to any part of the field of view of the considered sub-channel of the instrument. In order to select the sub-channel, STC was mounted in a thermal-vacuum chamber (TVC) on the side of the OGSE which could rotate along the vertical axis (z_{or} in Figure 2).

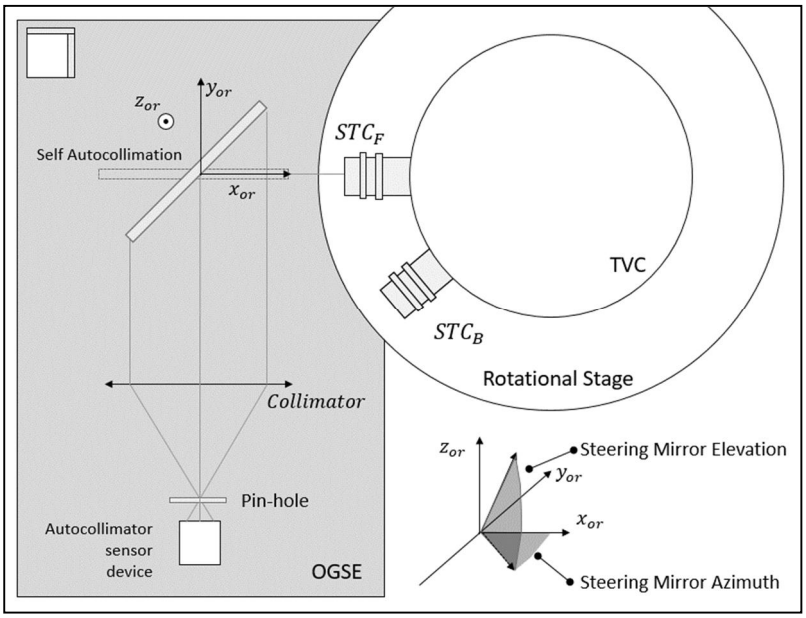

Figure 2. OGSE schematic diagram and reference system definition.

The stability of the performance of the OGSE is guaranteed by the high repeatability of the rotator stages which is less than 1 arcsec around z_{or} axis and 2 arcsec around the other axis direction. This high repeatability allows also to assure a good level of accuracy through a precise calibration of the stages done with a theodolite. The alignment between the optical bench and the Thermal Vacuum Chamber (TVC) was performed by a common alignment with gravity both for the Steering Mirror reference system and the TVC rotational stage.

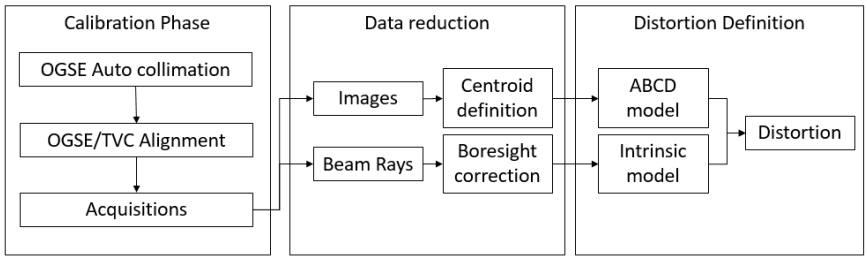

Figure 3. Flux diagram of the distortion map definition by using the OGSE.

As shown in Figure 3 the geometric calibration pipeline was divided mainly in three phases. During the first one, the OGSE has been aligned to the STC sub-channels and the acquisitions were carried out. The beam directions (measured by the steering mirror position) and images have been provided as output from this phase.
During the second phase, the background has been subtracted to the images and then the spot centroid positions on the images have been detected through a greedy algorithm. On the other side, the ray directions have been corrected through a rotation to compensate as better as possible the misalignment introduced in previous phases.
The last phase of the pipeline has been carried out by means of two different distortion model approaches: one commonly adopted for on-axis optical instrument calibration (the so called ABCD model) and the second one based on the Intrinsic Parameters (used in photogrammetry).
The final characterization of the distortion map of the stereo camera is the result of the two models.

4. DATA REDUCTION PHASE

The STC geometrical calibration is performed by measuring the centroid of the spot generated by a collimated beam focused on the detector by knowing accurately its orientation with respect to the camera axis. To minimize the effect of the readout noise of the detector (verified as a std around 10 DN at the nominal temperature), multiple acquisitions were commanded for each beam orientation. The pointing coordinates have been supplied as azimuth (az_M) and elevation (el_M) angles (see Figure 2) of the steering mirror. Each acquisition is defined in the reference system of the detector by the spot centroid coordinates (i_c, j_c).

4.1 Centroid definition

The beam projections on the image plane are shown in Figure 4. The beam dimension was defined by the pinhole aperture chosen to be 750 micron for practical reason: CMOS technology unfortunately presents a high Fixed Pattern Noise (FPN) (measured around 60 DN in nominal condition on the beam) which makes difficult to define the centroid as weighted mean of the image function on both the coordinates. Even if the preliminary subtraction of image background removes the Dark Signal Not Uniformity (DSNU), the Photo Response Not Uniformity (PRNU) generates an uncorrelated noise of about 150/200 DN (RMS value) depending on STC temperature (263.2 K in the "cold case" and 273.1 K in the "hot case"). The noise level increases in the beam light condition; it is measured to be around 350 DN at the nominal temperature (268.1 K). In order to limit the impact of this noise on the centroid measurements, it has been preferred to increase the spot size together with taking advantage of a recursive definition of the centroid defined by the boundaries of the spot (green line in Figure 4).
The starting identification of the centroid has been refined by a polynomial interpolation of all the radial sections of the image. These radial sections are modeled by means of a raised cosine filter and the half maximal threshold value has been chosen to define the border points. These points are recursively used to redefine the center of the spot (modelled as an elliptical shape) until stability is reached.

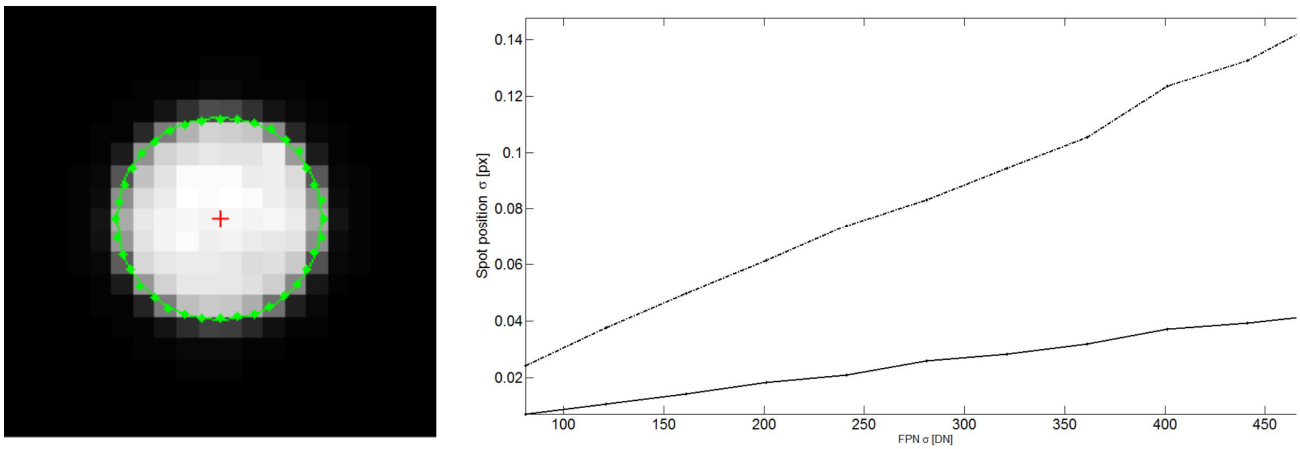

Figure 4. (a) Example of an image spot acquired for the geometrical calibration data set. The points which define the limits of the raised cosines have been marked in green and in red the final centroid position is shown. In (b) the error in the centroid determination estimated on a synthetic image with a classical centroid method (dotted line) and with a recursive approach (continuous line).

The approach considered has been validated by a synthetic modelling of the spots as radial raised cosine with a width of 4.6 pixels and a roll off factor of 0.4 pixel (as measured by calibration data) adding also an uncorrelated error (simulating the PRNU) as defined by the preliminary radiometric calibration measurements. A test of the accuracy of the centroid definition allowed to estimate an error of around 1/20 of the pixel (Figure 4b).
An example of the global centroids map on the image plane is shown in Figure 5.

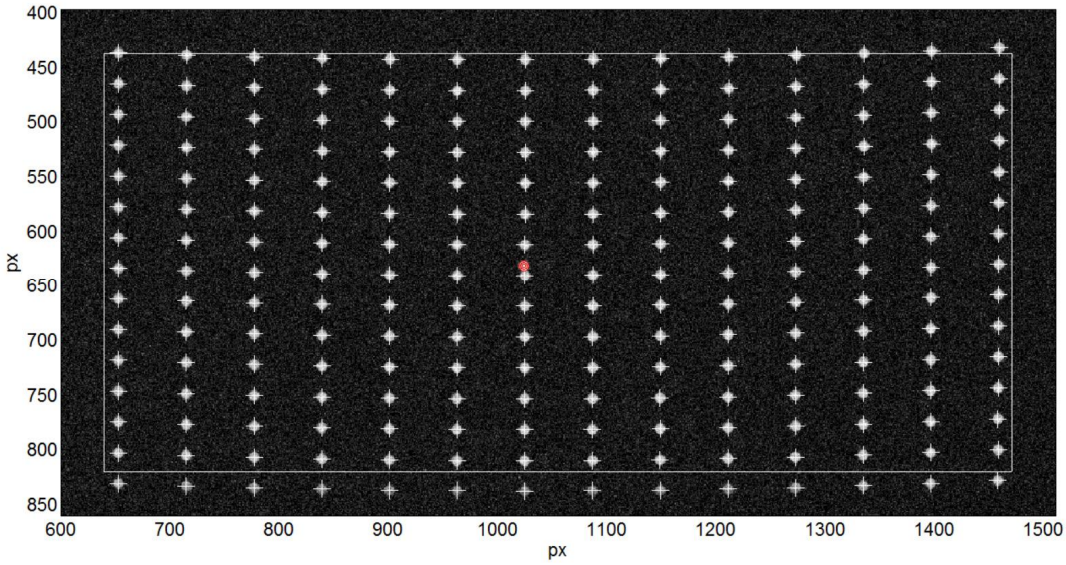

Figure 5. Averaged centroid map acquired during a session of the geometric calibration of the H-panchromatic filter of STC. White crosses identify the measured centroids and the lines define the nominal dimension of the filter. The red dot represents the optical definition of the boresight of the instrument.

4.2 Boresight correction

In order to perform a correct definition of the distortion corresponding to each centroid position, the corresponding optical ray versor has been defined in the reference system of the sub-channel boresight. This alignment could have been performed in the laboratory, but considering the time consuming procedure, an analytic optimization was preferred.
Considering the inclination of 45° of the steering mirror and that azimuth and elevation angles provided by OGSE housekeeping data are defined in the reference frame of the optical axis of the collimator, the cosine directors of the projected rays can be defined in the camera reference frame by the following equations:

$$\widetilde{v_i} = \begin{bmatrix} \sin(2\ az_{Mi})\cos(el_{Mi})^2 \\ 1 - 2\ (\cos(az_{Mi})^2)\cos(el_{Mi})^2 \\ \cos(az_{Mi})\sin(2el_{Mi}) \end{bmatrix}$$

All the resulting versors $\widetilde{v_i}$ are oriented on a reference system defined by x_{or} ; an additional correction has to be introduced to rotate them to a reference system aligned with the boresight direction $\widetilde{v_b}$ (see Figure 6).

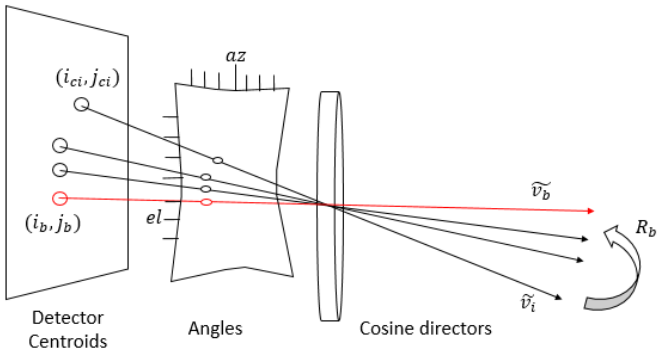

Figure 6 Figure shows the different associations between the different sets of data: centroid coordinates are associated to cosine directors which can be described by az and el angles. The reduction process for the definition of the distortion map required all the cosine directors in a reference system aligned with the boresight.

Considering the optical definition of the boresights (i_b, j_b) for the sub-channels on the image plane of the detector and the map between the centroids and the versors obtained by image reduction, the definition of the boresight vector $\widetilde{v_b}$ is computed by polynomial interpolation. The knowledge of this vector allows to define the minimal rotational matrix R_b to redefine all the versors $\widetilde{v_i}$ in a reference system aligned with the boresight.
The procedure applied to the High and the Low Panchromatic filters demonstrates the consistence of the data revealing a small misalignment between the TVC and the OGSE corresponding to 3.7e-3° with respect to y_{or} direction (cross track) and reporting an angle respect to the nadir direction of 21.37°.

5. CAMERA AND DISTORTION MODEL

The procedures described until now allowed to obtain the directions of the beams in the boresight centered reference system and to obtain, in the so-defined image plane, the beams coordinates from the projection that considers the versor directions. This two set of data can be considered to obtain the best model for the description of the optic proprieties of instrument. The off-axis configuration of STC and the necessity to derive a set of intrinsic parameters able to initialize a photogrammetric pipeline, addressed the definition of the distortion model and the ways to define the transformation parameters between the camera lens and the image planes.

5.1 Intrinsic matrix definition

The reconstruction of the three-dimensional structure of a scene from images relies on the laws of geometric optics and the optical lens systems are commonly described by the simple pinhole model.

The image formation process is determined by the intrinsic parameters of the camera, related to the lenses and the detector. For a camera described by the pinhole model and equipped by digital sensor, these parameters include the principal distance (focal length), the effective number of pixels along the horizontal and vertical axes, the pixel skew angle and the coordinates of the principal point in the image plane.
For the real lens systems, the image coordinates of the points acquired on the scene may deviate due to the effect of distortion.
A pinhole camera model is defined by a perspective transformation by a general non-singular linear transformation of homogenous coordinates. In particular defining as $\bar{u}$ the homogeneous coordinates on the image plane and $\bar{x}$ the homogenous coordinates in the world coordinate system, the pinhole camera model is defined by the projection matrix $P \in R^{3\times4}$ where

$$\bar{u} = P\,\bar{x} \tag{1}$$

Matrix P is defined as

$$P = K[R|-RC] \tag{2}$$

where:

C is the center of the projection (dual definition of the optical pupil of the instrument).
$R\ is$ the rotational matrix from the 3D reference frame to the projection axis of the instrument.
$K\ is$ the intrinsic matrix defined as follows (pixel quantization is not considered for better reading):

$$K = \begin{bmatrix} c_x & s & x_o \\ 0 & c_y & y_o \\ 0 & 0 & 1 \end{bmatrix} \quad (3)$$

Here c_x, c_y are the in the following pages called "*focal factors*" to avoid confusion with optical focal lengths along horizontal and vertical directions; s is the so called skew factor and $(x_o y_o)$ represent the coordinates of the principal point (as in the computer vision literature [21]).

This model completely describes a camera model in the reference system of the projection axis (the principal axis orthogonal to the image plane).
As we will see in the next section, this model can be considered as the result of a linear approximation with respect to an ideal central pinhole camera in which the projection can be described by a unique *focal factor*, the focal length.

As described in Section 0, STC has an off-axis optical configuration which defines the distortion map of the instrument as not telecentric. Since the main aim for STC is to reconstruct the surface of Mercury in 3D by a photogrammetric pipeline, the precise and robust definition of the intrinsic parameters becomes very important. The strong correlation between the parameters defining the camera model is high because of the optical configuration (long focal length and small dimension sensor. The characterization of the distortion model becomes relevant for a consistent definition of the focal length and of the principal point position, that are so important in the initialization of the photogrammetric process. With this aim, two different approaches have been developed and analyzed.

A common optical approach is based on the so called ABCD matrix and reduces the camera model to a perspective model with a unique focal length. This approach has the advantage to allow the characterization of a camera model with three values: the two boresight coordinates on the focal plane and focal length. On the other side, the distortion map is not so accurate introducing an increasing of the interpolation effect on the final results for geometrical calibration.
The definition of the intrinsic parameters (to be introduced into the photogrammetric pipeline), on the other side, aims to describe with minimal residuals the geometry of the projection system but needs the definition of five parameters in order to identify the transformation between the optics and the image plane, and the so defined reference system has no physical correspondence for an instrument with so complex optical design.

The next section has the aim to solve part of this misalignment between the two approaches. The central pinhole model (a unique focal factor in both the directions) will be introduced. It will be shown how this model can be linearly approximated in an arbitrary point both using the $ABCD$ model or the intrinsic parameter matrix (camera calibration matrix).

5.2 Pin-hole model and principal point

All the pinhole cameras can be described by an image plane and a projection center C. The projection ray, which is orthogonal to the image plane (Figure 7a) intersects it in the central point x_c. We will consider this axis as principal central axis.
In a reference system aligned with the central axis, two points on the focal plane symmetric with respects the central point define the same angle with respect to the projection axis. In other words, all the projection rays with the same angular distance with respect to the central axis identify a circle on the image.
The distance between the image plane and the projection center (the so called focal flange or principal distance) represents the focal length. Only in this case, in the reference system of the central axis, we can write:

$$K_c = \begin{bmatrix} f & 0 & x_c \\ 0 & f & y_c \\ 0 & 0 & 1 \end{bmatrix} \rightarrow \begin{bmatrix} \bar{u} \\ 1 \end{bmatrix} \parallel K_c \; x \rightarrow \begin{bmatrix} \bar{u} \\ 1 \end{bmatrix} = K_c \; \bar{t} \quad (4)$$

Here $\bar{t}$ represents the homologues vector of the tangents of the angles α_x, α_y, the horizontal and vertical angles which define the projected point x. In this reference system the perspective can be seen as a linear process between the tangents of the angles and the image coordinates.

In a telecentric ideal camera, the central axis corresponds to the boresight of the instrument. In a real camera the focal lengths in the two directions are not equal. This can be easily described by a rotation of the reference system with respect to the central one. In a different reference system in fact, the projection becomes not linear with respect to the tangents of the angles but it can be approximated defining two different focal lengths in the two directions.
The rotation around an axis of an angle θ (Figure 7b), for instance, can be described by a new pinhole model defined on a different point (in the image x_b) with an increased *focal factor* equal to $\frac{1}{\cos(\theta)^2}$.

(a) (b)

Figure 7 In (a) description of the ideal pinhole camera. The projection center C is defined with the point x_c at its minimal distance (principal distance) from the image plane. Considering a point x_b, the prospective model in this new reference system can be approximated with a new pinhole model with two different *focal factors* in the horizontal and vertical directions. In (b) a simplified model in which the rotation is around one axis. The distance between prospective center and x_b increases by a factor $\frac{1}{\cos(\theta)}$. In this direction the new *focal factor* increases for its square while in the other direction it remains f.

Considering that the ideal model is not realizable, we start from it and we will see how in a different reference system (centered on a different point of the image plane) the pin-hole model can be approximated.
We consider an arbitrary rotation R_{bc} to move the axis from x_b to x_c.
As shown in Figure 7, R_{bc} can be defined as a function of its z-x-z proper Euler angles $(\vartheta, \theta, \psi)$, where ψ defines the rotation to align the two points on the x axis, θ represents the angle between the direction of x_b considered and the central axis, while ϑ (rotation around the new perspective axis) is left free.
Through this convention, the new point x_b can be written as:

$$x_b = x_c + f\tan(\theta)\begin{bmatrix}\sin(\psi)\\ -\cos(\psi)\end{bmatrix} \tag{5}$$

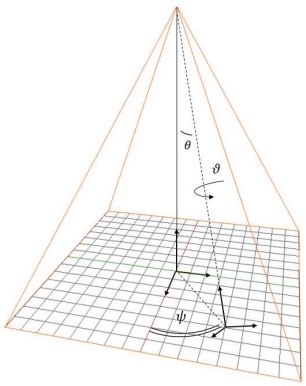

(a)

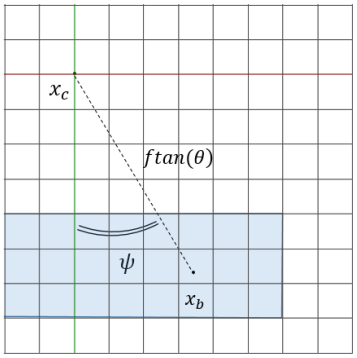

(b)

Figure 8 . Description of the z-x-z proper Euler angles. Approaching to the transformation in opposite sense, the rotation to move from x_c to a image plane point x_b can be described as a rotation on the central axis of an angle ψ followed by a rotation to reach the second point with an angle θ. Last rotation ϑ (around new perspective axis) is not restricted. On the image plane this angle brings to a movement of a distance $ftan(\theta)$.

The resulting projection system, in the new reference system x', can be described as:

$$\begin{bmatrix}\bar{u}\\1\end{bmatrix} \parallel K_c\, R_{bc}\, x' \rightarrow \begin{bmatrix}\bar{u}\\1\end{bmatrix} = \frac{K_c\, R_{bc}\, x'}{r_3 x'} \rightarrow \bar{u} = F_{R_{bc}}(\bar{t}\,') \tag{6}$$

The third line of rotation matrix r_3 represents the central axis of the system in the new reference system.
In this reference system the process is no longer linear, but it is described by a function depending by the tangents $\bar{t}'$ and by the rotational matrix R_{bc} . This function can be approximated with a Taylor development at the first order.
We can approximate the transformation as:

$$\bar{u} = F_{R_{bc}}(\bar{0}) + \frac{\partial F_{R_{bc}}}{\partial \bar{t}'}(\bar{0})\, \bar{t}' \rightarrow \bar{u} = T_{ABCD} \begin{bmatrix}\tan(\alpha_x')\\ \tan(\alpha_y')\end{bmatrix} + x_b \tag{7}$$

where T_{ABCD} is the so called $ABCD$ matrix and it is function of the $(\vartheta, \theta, \psi)$ angles. In a calibration system, the knowledge of the perspective ray direction in the optical system reference frame and the coordinate on the image plane reference one permits to estimate easily this matrix which is unique considering the defined reference system.

$$T_{ABCD} = F(f, \theta, \psi, \vartheta) = \begin{bmatrix} f_x & s_{xy} \\ s_{yx} & f_y \end{bmatrix} \tag{8}$$

The classical approach for an on axis instrument foresees to consider the focal length of the instrument as the mean of the diagonal terms of this matrix and considers as distortion the element on the opposite diagonal. This model is simple and allows to describe with few parameters an off-axis projection in an arbitrary reference system. A common choice is represented by the boresight of the instrument.

If we consider the conventions adopted in a general mathematic framework of projective geometry commonly defined in a photogrammetric pipeline, some constraints have to be introduced. A new constraint has to be added to the definition of the rotation R_{bc}, imposing the ϑ angle in order to obtain a reference system where the y axis is aligned to the central reference system on the image plane. This strategy permits to nullify the C term of the T_{ABCD} matrix and it results:

$$T_{y0} = f\frac{\cos(\vartheta)}{\cos(\theta)^2}\begin{bmatrix}\frac{\cos(\theta)}{\cos(\psi)} & -\sin(\psi)\sin(\theta)^2 \\ 0 & \frac{\cos(\psi)}{\cos(\vartheta)^2}\end{bmatrix} \quad (9)$$

Summarizing, considering an arbitrary point x_b defined by angles θ, ψ in the equation (5), the perspective model can be approximated in its reference system associated as a linear approximation through T_{y0} matrix. The process can be inverted: that means that knowing T_{y0} matrix, defining the original center position becomes possible.

The resulting projection matrix K is described by:

$$K = \begin{bmatrix}T_{y0} & x_b \\ 0\ \ 0 & 1\end{bmatrix} = \begin{bmatrix}\mathrm{c_x} & s & x_b \\ 0 & \mathrm{c_y} & \mathrm{y_b} \\ 0 & 0 & 1\end{bmatrix} \quad (10)$$

The point where the linear approximation is minimum is considered as principal point. In a projection system this point is unique. In its reference system, equation (10) provides the intrinsic parameters matrix of the camera that is commonly used in the pipeline for the image processing. The values c_x, c_y are considered the horizontal and vertical *focal factors* and s (null for an ideal camera) is called skew factor and is classically described, for simplicity, as the not orthogonality of the pixel grid of the detector.

The knowledge of the direction of the projective rays, in a known reference system, and the projected coordinates of the image plane permits, by a projection process, the inversion and QR-decomposition to estimate both the intrinsic matrix K and the rotation R to move from the reference system considered to the principal one.

6. STC DISTORTION MODEL

In Table 3 the result of the classical T_{ABCD} model and the Camera matrix (that maps the points in the OGSE reference system to the image plane) is reported.
As described before, the first model linearizes the perspective on a defined point (the boresight of the instrument). After this minimization process the mean of the focal length is computed permitting to define the camera model that can be simply described by three parameters: the mean focal length and the coordinates of the boresight.
The second approach is certainly more verbose: it describes the camera by two matrices. A rotational matrix to bring the reference system in the principal point reference system and the intrinsic parameter matrix which defines the focal lengths, the position of the principal point and the skew factor.
A further step is done in this context by the inversion of the intrinsic matrix. The intrinsic matrix permits univocally to define the dual central point in which the horizontal and vertical focal lengths are equal. In this reference system, as in the T_{ABCD} model, the pinhole camera can be described by only three parameters: focal flange and the coordinates position of the central point.

6.1 ABCD Model Reduction

Figure 9 shows the definition of the distortion maps of the two channels of STC considering the pinhole model defined by T_{ABCD} matrix. Considering that this approach defines the focal length as the mean of the horizontal and vertical focal lengths, the resulting residual distribution, considering the off-axis configuration, results unbalanced and along track residual results are larger than the cross-track ones.

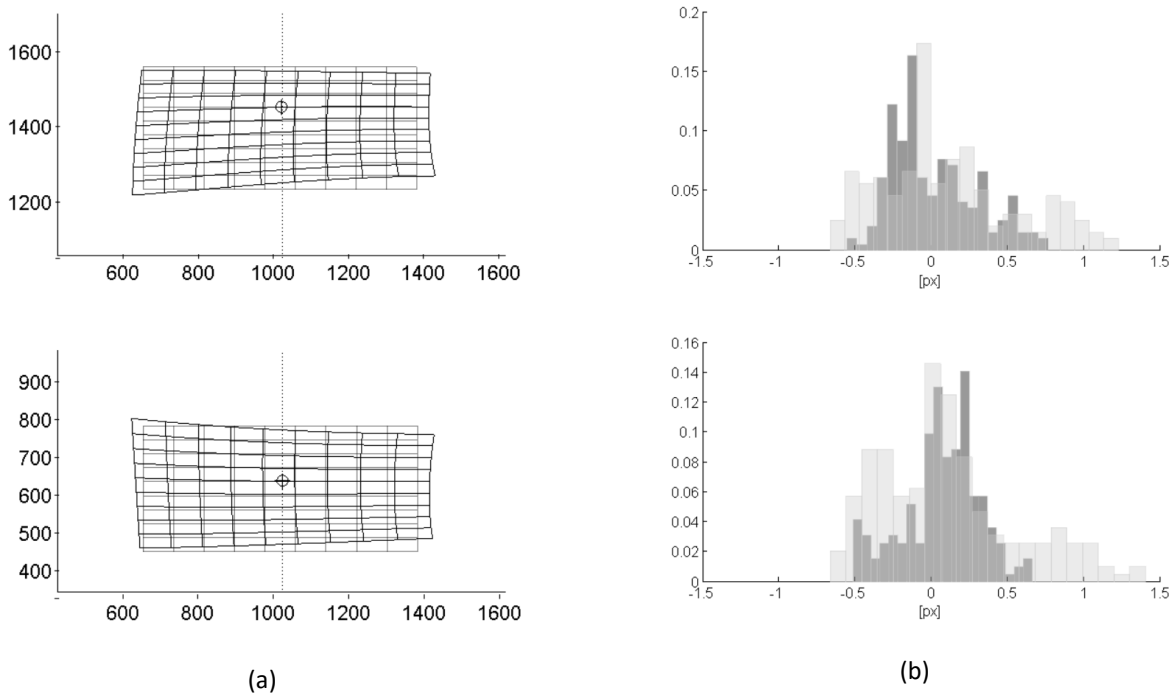

Figure 9 . In (a) distortion map at nominal temperature for both the STC sub-channels (respectively Low and High) as obtained by the application of the T_{ABCD} classical model. The two grids represent the nominally projected equally spaced grid and the imaged one, where the differences between the two are increased by a factor 50. Axes represent positions in pixel in detector reference system. The boresight positions are marked with a crossed circle. In (b) residual distribution for the two channels in pixels and μm.

Both the instrument channels present in this model a mean focal length on the boresight of 95.275 mm. The horizontal focal length results around 95.4 mm while horizontal around 95.1 mm (see Table 3). The substantial difference between the not diagonal coefficient of the two channels is due to the asymmetric configuration of the instrument as described in the following section.

Table 3. Pinhole intrinsic model of STC from calibration data distortion model. These parameters define the intrinsic matrix defined in Session 5. In particular, the focal lengths have to be considered as the *focal factors* of the instrument centered on the principal point with vertical axis aligned with optical one. The three angles define the rotation between the reference system of the boresight and the principal point one.

	PANH		PANL	
	Along track	Cross track	Along track	Cross track
Boresight [pxl]	629	1025	1452	1022
T_{ABCD} [mm] centered on boresight	95.4300	-0.0650	95.4348	0.6126
	0.1066	95.1099	-0.7004	95.1231
Mean focal length [mm]	95.27		95.2812	

As result of this approach which has the strong advantage to parametrize the camera model with only three coefficients and to be describable in the reference frame of the boresight of the channel, the distortion model resulting has a maximal radial and tangential distortion of 1.5 pixels which represent, as predicted [8], a distortion of the 0.3% on the external part of the field of view. Residuals present a mean RMS of 0.37 px.

6.2 Intrinsic parameters approach reduction

In this context, a second model more appropriate for an off-axis configuration is proposed . The pinhole perspective matrix definition permits to define the camera model using five parameters and a rotation matrix to move on the principal point. It has to be considered that, as explained before, the intrinsic matrix can be reduced (as in the case of ABCD case) to a matrix with a unique focal value, the focal flange, as long as the reference system is taken back to the central projection system. This model, as the previous one, needs only three parameters, but it requires to be centered in a reference system that has not a common use and for an off axis instrument like STC it is centered out of the field of view.

The data reduction results for projective model are reported in Table 4.

Table 4. Pinhole intrinsic model of STC from calibration data distortion model. These parameters define the intrinsic matrix defined in Session 5. In particular the focal lengths have to be considered as the *focal factors* of the instruments centered on the principal point with vertical axis aligned with optical one. The three angles define the rotation between the reference system of the boresight and the principal point one.

	PANH		PANL	
	Along track	Cross track	Along track	Cross track
Principal points [pxl]	893.0995	1059.9441	1188.1287	1061.9443
Focal factors [mm]	95.31	95.08	95.37	95.11
Skew factor	-11.27		6.93	
Focal Flange	94.84		94.81	
Rotation respect principal axis (ka)	-0.4354°		0.0017707°	
Rotation around cross track direction (phi)	-1.5805°		1.5939°	
Rotation around long track direction (om)	-0.23495°		-0.21474°	

As described previously, the principal points are shifted with respect to the center of the detector in both the directions due to the off-axis configuration. As expected, a rotation of 0.43° is measured between the two sub-channels. This rotation is due to the fact that the geometric distortion of the instrument would have to be distributed symmetrically on the two channels as opposite rotational angle. During the mounting phase it was preferred to align precisely one of the sub-channels (the Low pancromatic one, which is considered the reference channel of the instrument) in order to have a more comfortable reference system for the instrument. The reference system in fact results aligned with the optical one with a precision of 1.7 arcsec. As consequence, the alignment has discharged a rotation on the other channel. The other three angles (showed in the table 4) defines the rotational matrix to move from boresight reference system to principal point one.

The inversion of the intrinsic parameters permitted to estimate the central reference system and so to define the Focal Flange (the principal distance of the ideal centered model for the two channel). The camera results symmetric (in the limit of the error band of the measurement) presenting for both the channels a value of about 94.8 mm. This distance does not represent the focal length of the instrument. The central distance as described in Section 5.2 has to be scaled to the boresight reference system where, for both the channels, is evaluated as 95.3 mm in along-track direction and 95.1 mm in cross track direction. This model represents the pinhole model which minimizes the distortion over the whole field of view of the stereo camera. The model, even by using a decentered reference system, allows to reach a distortion map limited to 0.2% both for radial and tangential directions with a standard deviation of the residual of 0.2 px. A maximum difference between model and data is guaranteed around 0.4 pxls with a residual RMS of 0.17 px (Figure 10). Considering the main aim of STC and the importance in the definition of the intrinsic parameters, the possibility to define the model of the telescope reducing of a factor 3 the distortion would allow to reduce the effect of the interpolation, preserving the image contents since the generic photogrammetric pipeline needs a further source of interpolation during the orthorectification of the images.

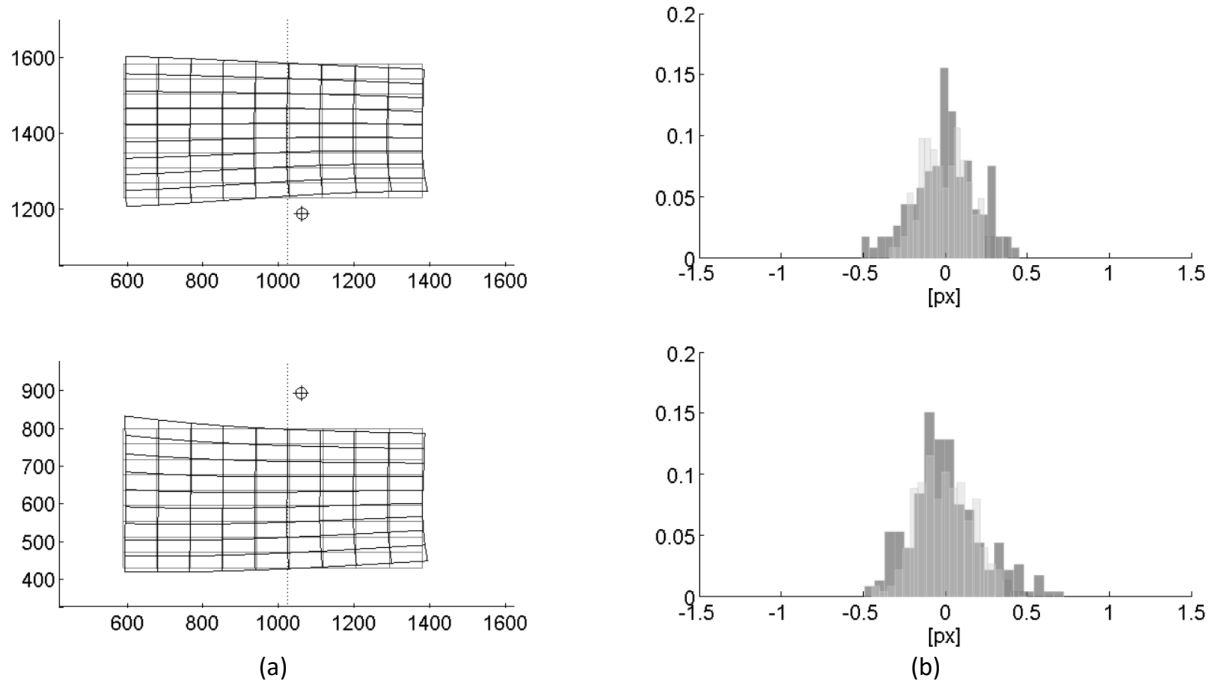

Figure 10 . In (a) distortion map at nominal temperature for both the STC channels (respectively Low and High) as obtained applying the Intrinsic Matrix based model. The two grids represent the nominally projected equally spaced grid and the imaged one where the differences between the two are increased by a factor 50. Axes represent positions in pixel in detector reference system. The principal point position is marked with a crossed circle. The vertical shift of the points can be linked to the along-track convergence rays configuration, while the horizontal one is due to the different focal lengths. In (b) residual distribution for both sub-channels in pixels and μm.

6.1 Parameters accuracy

A validation analysis of the stability of the model has been performed by considering the propagation of the noise in the bench of data. As source of noise the centroid definition has been considered, the repeatability of the rotational stage of the TVC, also the repeatability of the steering mirrors (in both the directions) and, last but not least, the thermal variation of the OGSE (negligible during an acquisition session but sensible between different days of calibration). For simplicity, the noise propagation has been simulated on the centroids assuming that the accuracy in the repeatability of the steering mirror rotation stages could be considered on the image plane. A white noise with a second order moment between 0 and 0.5 pxl is so propagated on the input data. Result of this test are shown in Figure 11.

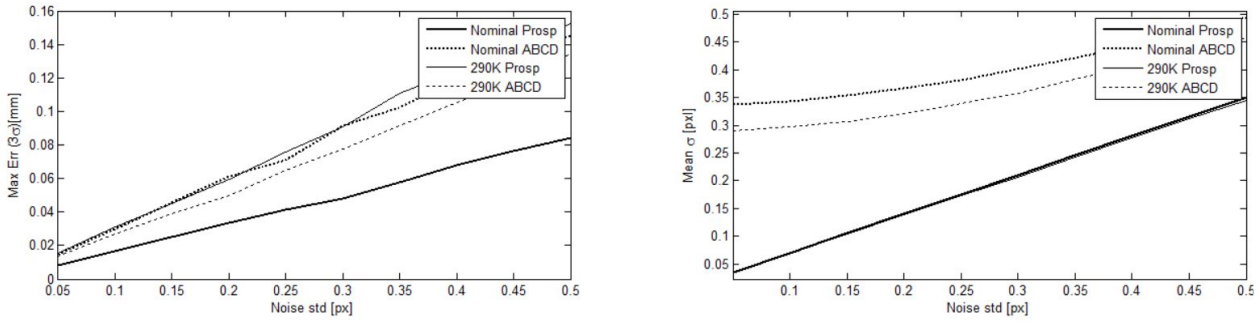

(a) (b)

Figure 11. In (a) propagation of the noise on the repeatability (evaluated as 3σ) of the measurements for the *focal factors* (continuous lines) and for the focal lengths (dotted lines) considered in the model definition for two test sessions (the nominal temperature session and the ambient temperature one). In (b) standard deviation of the residual for the two models and the two sessions always as a function of the noise error defined on the image plane.

The tests demonstrated the repeatability of the measurement. In particular, for the test session with a grid of 15x15 spot, the *focal factors* in both the directions are estimated with an error bar less than 0.05% and 0.1% for the ABCD model. Worst results are obtained for the second proposed test in which the source of error are larger. In this case, high temperature and a 9x9 points grid make the perspective information not more less incident. In both the cases (see Figure 11b) the residual are particularly low for the perspective model.
It has to be considered that perspective *focal factors* high accuracy is justified by the correction of the principal point in each session. Deeper analyses have to be performed to identify the impact of this solution in terms of correlation between principal point coordinates and the other parameters of the camera model.

6.2 Temperatures

Different investigations are nowadays in progress to define the thermal model of the instrument. Through the use of the two proposed models, the main idea is to define a temperature depending pinhole camera model and distortion map model. An example of the evaluation currently underway is presented in Figure 12, where an estimation of the *focal factors* and of the focal lengths is proposed. It is worth noting that the ratio of these couples of values can be associated to the incident angle between the channel optical path and the one of the Schmidt portion of the instrument (considered at Nadir) which reaches, as expected by the ambient mounting temperature, the expected value of 3.75°.

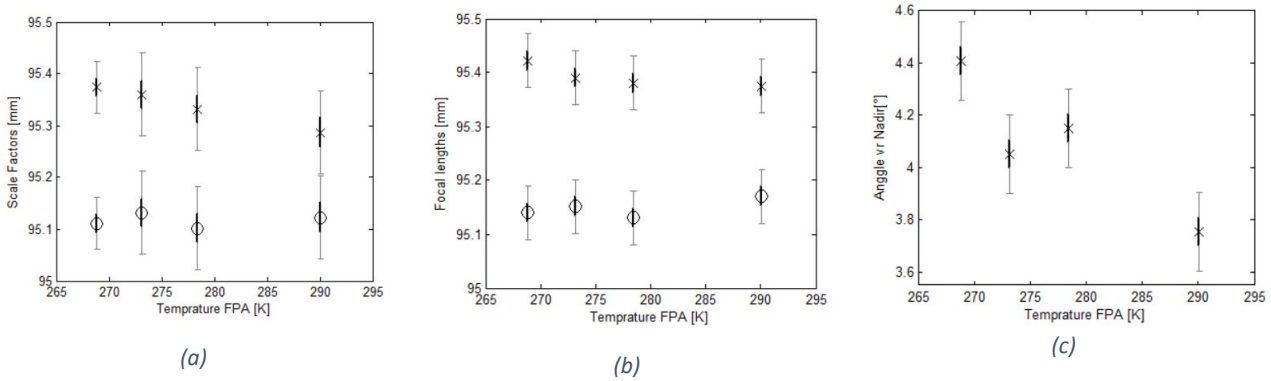

(a) (b) (c)

Figure 12 Dependency of the focal lengths on the temperature of the FPA for both the models considered for the reference Low panchromatic channel of the camera. In (a) the perspective intrinsic model and in (b) the $ABCD$ one. In (c) the evaluated angle of the optical channel with respect to the nadir direction. All sessions acquired are shown with the error bar associated to the measurement. In black the σ and in gray the 3σ bar. More precise measurements have been acquired at the 268 K nominal temperature for the stereo camera.

Different analyses have to be performed to define the variability of the instrument with the temperature. A deformable pinhole model of the cameras, based on the definition of the variability of the parameters considered, could be used to minimize the variability of the distortion map. At the temperature considered, a definition of the pinhole model referred on the same reference system, has been performed. The resulting distortion maps have a misalignment of 0.1 pxl cross track and 0.2 pxl along-track with respect to the ones presented in Section 6.2.

7. CONCLUSIONS

This paper proposes a distortion model the Stereo Camera STC in the context of ESA BepiColombo mission. The novel design of the telescope presents an off axis configuration which leads to develop a new approach in the definition of the distortion map. Two different models, one commonly applied in optics and the other one generally used for photogrammetric pipelines, are proposed. The two approaches, as demonstrated, can be reduced into a unique approximated model. Performance comparisons have been analyzed for both the models. The results obtained during the calibration campaign are presented showing that both distortion models are quite accurate. The classical distortion model is presented in a classical optical form and it presents a maximum value around 0.3%. The approach, based on ABCD matrix can rescue a comfortable model with an on axis distortion map. The second proposed model has been developed following the conventions used in the photogrammetric approaches and allows to have a less approximated model of the camera (for an off axis instrument) reducing the distortion to a factor 1/3 with respect to the previous case. A disadvantage of this approach is the use of a reference system not based on a physical axis and the verbosity of the quantity of parameters adopted to define the camera model. However, it has the significant advantage of reducing the use of interpolation before the 3D reconstruction pipeline so potentially allowing to reach better results considering that classical stereoscopic pipeline needs anyway an additive interpolation due to images rectification.

However, it has the advantage of reducing further sources of interpolation beyond the one performed during the ortho-rectification.

8. ACKNOWLEDGMENTS

This activity has been realized under the BepiColombo Agenzia Spaziale Italiana (ASI) contract to the Istituto Nazionale di Astrofisica (INAF I/022/10/0) and with the support of Leonardo company (Campi di Bisenzio (FI) – Italy).

REFERENCES

1. J. Benkhoff, J. van Casteren, H. Hayakawa, M. Fujimoto, H. Laakso, M. Novara, P. Ferri, H. R. Middleton and R. Ziethe, “BepiColombo - Comprehensive exploration of Mercury: Mission overview and science goals”, *Planet. Space Sci.*, vol. 58(1-2) 2-20, (2010).
2. J. Benkhoff, “The BepiColombo Mission to explore Mercury - Overview and mission status”, *44th LPSC*, 2834 (2013).
3. J. Benkhoff, “The BepiColombo MPO”, *38th COSPAR Scientific Assembly*, 18-15 July 2010 Bremen (Germany), 2 (2010).

4. H. Hayakawa, Y. Kasaba, H. Yamakawa, H. Ogawa and T. Mukai, "The BepiColombo/MMO model payload and operation plan", *Advance in Space Research*, vol. 33, pp. 2142-2146 (2004).
5. N. Thomas, T. Spohn, J.-P. Barriot, W. Benz, G. Beutler, U. Christensen, V. Dehant, C. Fallnich, D. Giardini, O. Groussin, K. Gunderson, E. Hauber, M. Hilchenbach, L. Iess, P. Lamy, L.-M. Lara, P. Lognonné, J.J. Lopez-Moreno, H. Michaelis, J. Oberst, D. Resendes, J.-L. Reynaud, R. Rodrigo, S. Sasaki, K. Seiferlin, M. Wieczorek and J. Whitby, "The BepiColombo Laser Altimeter (BELA): Concept and baseline design", *Planet. Space Sci.*, vol. 55(10), pp. 1398-1413 (2007).
6. Zhang Z., "A flexible new technique for camera calibration", IEEE Transactions on Pattern Analysis and Machine Intelligence, 22(11), 1330-1334 (2000).
7. E. Flamini, F. Capaccioni, L. Colangeli, G. Cremonese, A. Doressoundiram, J.L. Josset, Y. Langevin, S. Debei, M.T. Capria, M.C. De Sanctis, L. Marinangeli , M. Massironi, E. Mazzotta Epifani, G. Naletto, P. Palumbo, P. Eng, J.F. Roig, A. Caporali, V. Da Deppo, S. Erard, C. Federico, O. Forni, M. Sgavetti, G. Filacchione, L. Giacomini, G. Marra, E. Martellato, M. Zusi, M. Cosi, C. Bettanini, L. Calamai, M. Zaccariotto, L. Tommasi, M. Dami, J. Ficai Veltroni, F. Poulet, Y. Hello and The SIMBIO-SYS Team, "SIMBIO-SYS: The spectrometer and imagers integrated observatory system for the BepiColombo planetary orbiter", *Planet. Space Sci.*, vol. 58, 125-143, (2010).
8. V. Da Deppo, G. Naletto, G. Cremonese, and L. Calamai, "Optical design of the single-detector planetary stereo camera for the BepiColombo European Space Agency mission to Mercury", *App. Opt.*, vol. 49(15), 2910-2919, (2010).
9. E.Simioni, V.Da Deppo, G.Naletto, G.Cremonese "Stereo Camera for satellite application: A new testing method" *Metrology for Aerospace (MetroAeroSpace)*,582-587, (2014).
10. Da Deppo V.; Naletto G.; Borrelli D.; Dami M.; Ficai Veltroni I.; Cremonese G., *"Indoor Calibration for Stereoscopic Camera STC, A New Method"* ICSO 2014 International Conference on Space Optics, (2014).
11. G. Marra, L. Colangeli, E. Mazzotta Epifani, P. Palumbo, S. Debei, E. Flamini and G. Naletto, "The optical design and preliminary optomechanical tolerances of the high resolution imaging channel for the BepiColombo mission to Mercury", *Proc. SPIE 6273*, 6273-28 (2006).
12. F. Capaccioni, M. C. De Sanctis, G. Filacchione, G. Piccioni, E. Ammannito, L. Tommasi, I. Ficai Veltroni, M. Cosi, S. Debei, L. Calamai, and E. Flamini, "Vis-Nir Imaging Spectroscopy of Mercury's Surface: Simbio-Sys/Vihi Experiment Onboard the Bepicolombo Mission", *IEEE Transactions on Geoscience and Remote Sensing*, vol. 48, 3932-3940, (2010).
13. Klaus Gwinner, et al, "Derivation and Validation of High-Resolution Digital Terrain Models from Mars Express HRSC Data", Photogrammetric Engineering and Remote Sensing 75(9):1127-1142 · (2009).
14. V. Da Deppo, G. Naletto, P. Nicolosi, P. Zambolin, M.G. Pelizzo, C. Barbieri, "Optical performance of the Wide Angle Camera for the Rosetta mission: preliminary results", in UV/EUV and Visible Space Instrumentation for Astronomy and Solar Physics, SPIE Proc. 4498, 248-257 , (2001)
15. C.Capanna et al, "Multi-Resolution Stereophotoclinometry by Deformation, a New 3D Shape Reconstruction Method Applied to ROSETTA/OSIRIS Images" The Visual Computer: International Journal of Computer Graphics, 825-835, (2013)
16. G. Naletto, V. Da Deppo, M. Pelizzo, R. Ragazzoni, and E. Marchetti , "Optical design of the Wide Angle Camera for the Rosetta mission" pp 1446-53, (2002)
17. S. Edward Hawkins III, "In-flight performance of MESSENGER's Mercury Dual Imaging System". Proc. SPIE 7441, Instruments and Methods for Astrobiology and Planetary Missions, (2009).
18. V. Da Deppo, G. Naletto, G. Cremonese, L. Calamai, R. Paolinetti, S. Debei and E. Flamini, "Optical design performance of the stereo channel for SIMBIOSYS onboard the BepiColombo ESA mission", in Proceeding of the '8th International Conference on Space Optics', Rhodes - Greece, 4-8 October 2010, (2010).
19. V. Da Deppo, G. Cremonese, G. Naletto, "Ghost images determination for the stereoscopic imaging channel of SIMBIOSYS for the BepiColombo ESA mission", SPIE 8167, Optical Design and Engineering IV, 81671U, (2011).
20. E. Simioni , C. Re , V. Da Deppo, G. Naletto, D. Borrelli , M. Dami , I. Ficai Veltroni , G. Cremonese , "Indoor calibration for stereoscopic camera STC, a new method", ICSO, vol 7, 10, (2014)
21. Hartley, R., Zisserman, A, "Multiple View Geometry in Computer Vision (2nd Edition)". Cambridge University Press, Cambridge,(2004)

22. C. Re ,E. Simioni, G. Cremonese , R. Roncella , G. Forlani , Vania Da Deppo , G. Naletto , G. Salemi, "DTM generation from STC-SIMBIO-SYS images" Proc. SPIE 9528, Videometrics, Range Imaging, and Applications XIII, (2015).